energies

MDPI

Article

Comparative Study on Artificial Fracture Modeling Schemes in Tight Reservoirs—For Enhancing the Production Efficiency of Tight Oil and Gas

Yonggang Wang [1,2], Xuejuan Zhang [3,*], Jie Zhang [1,2], Yali Zeng [1,2], Lei Zhang [3], Han Wang [3] and Ruolin Li [3]

[1] Research Institute of Exploration and Development, Changqing Oilfield Company, PetroChina, Xi'an 710018, China; wangyg_cq@petrochina.com.cn (Y.W.); zhangjie161@mails.ucas.ac.cn (J.Z.); zengyl1_cq@petrochina.com.cn (Y.Z.)
[2] State Engineering First Laboratory of Low Permeability Oil Field Exploration and Development, Xi'an 710018, China
[3] College of Petroleum and Natural Gas Engineering, Chongqing University of Science and Technology, Chongqing 401331, China; 2019013@cqust.edu.cn (L.Z.); 2022201114@cqust.edu.cn (H.W.); 2023201024@cqust.edu.cn (R.L.)
* Correspondence: zhangxuejuan_2006@126.com

Abstract: In order to improve the reliability of the deployment of production schemes after artificial fracturing in tight reservoirs, it is urgent to carry out research on the description of fractures after artificial fracturing. In this study, taking the Chang 6_1 oil formation group in the Wangyao South area of Ordos Basin as an example, three different fracture modeling schemes are used to establish the geological model of fractured reservoirs, and the fitting ratios of the respective reservoir models are calculated by using the method of reservoir numerical simulation of the initial fitting, and the optimal fractured reservoir modeling scheme is screened in the end. The research area adopts three types of fracture prediction results based on FMI fracture interpretation data, seismic fracture prediction data, and rock mechanics artificial fracturing simulation data. On this basis, geological models of fractured reservoirs are established, respectively. The initial fitting of reservoir values of each geological model are compared, and the highest initial fitting rate of reservoir values is 88.44%, which is based on rock mechanics artificial fracturing simulation data. However, the initial fitting rate of the reservoir model was the lowest at 75.76%, which was established based on the fracture random modeling results of FMl fracture interpretation data. Under the constraints of seismic geostress prediction results and microseismic monitoring data, the simulation results of rock mechanics artificial fracturing fracture are used as the basis, on which the geological model of artificially fractured reservoirs is thus established, and this scheme can more realistically characterize the characteristics of fractured reservoirs after artificial fracturing in the study area.

Keywords: tight reservoir; artificial fracturing; fracture prediction; reservoir modeling

Citation: Wang, Y.; Zhang, X.; Zhang, J.; Zeng, Y.; Zhang, L.; Wang, H.; Li, R. Comparative Study on Artificial Fracture Modeling Schemes in Tight Reservoirs—For Enhancing the Production Efficiency of Tight Oil and Gas. *Energies* **2024**, *17*, 5235. https://doi.org/10.3390/en17205235

Academic Editor: Reza Rezaee

Received: 29 August 2024
Revised: 7 October 2024
Accepted: 16 October 2024
Published: 21 October 2024

1. Introduction

In low permeability reservoirs, artificial fracturing technology should be used to improve the physical properties of the reservoirs, so as to realize the effective development of tight oil and gas reservoirs. The distribution characteristics of artificially induced fractures will directly impact the dynamic production behavior of the oil field. The fine portrayal and establishment of artificial fracture characteristics after fracturing can reflect the fine geological model of fractured reservoirs with seepage characteristics of reservoirs after artificial fracturing. Therefore, it is an urgent practical problem to improve the development efficiency of tight reservoirs after fracturing [1,2].

Dershowitz, B. [3] and others argued that in real reservoirs, fracture network models are more consistent with fracture non-homogeneity and connectivity. Sarda, S., Jeannin,

L. [4] et al. defined fracture nodes according to fracture intersections and ends. Jian, W. [5] et al. used imaging logging and dynamic monitoring data, etc., to quantitatively characterize the geometric parameters of the fractures. Fracture network model characterization theory and technology are important technical support for artificial fracture characterization [6,7]. However, there is a big difference between geological modelling of artificially fractured reservoirs and naturally fractured reservoirs coarse, which is reflected in the data, information, and its technical methods. The reservoir geological modeling methods adopted in different study areas are different, and the optimal reservoir geological modeling scheme should be selected according to the target reservoir, structural conditions, the richness of original data, and the particularity of the data [8,9].

Chang 6_1 oil reservoir in the Wangyao South area of Ordos Basin, which contains low porosity and low permeability reservoirs, is a reservoir with strong heterogeneity and undeveloped natural fractures. Based on the characteristics of the fracture information data source after artificial fracturing, the corresponding fracture modelling methods are selected, and finally different artificial fracture modelling schemes are obtained. By comparing the initial fitting rates of geological models for different fractured reservoirs, the optimal modeling scheme for artificial fractured reservoirs in the study area is selected

2. Materials and Methods

Fracture properties of fractured reservoirs can be described through two parts: reservoir matrix and fracture. Petrel combines both the discrete fracture network (DFN) model and implicit fracture model (IFM) into standard fracture modeling with a hybrid model. In the discrete fracture network (DFN) model, large/significant fractures are explicitly modeled as discrete slices. In the implicit fracture model (IFM), grid properties represent the subtle part of the distribution of fracture properties (smaller fractures), i.e., reservoir matrix properties [10].

In this study, the implicit fracture model (IFM) was used to characterize the tight reservoir matrix property model, and the discrete fracture network model (DFN) was used to characterize the artificially fractured fracture model. Ultimately, it is synthesized in the form of attribute models such as permeability and porosity, which can reflect the information of both in an integrated geological model of fractured reservoirs.

2.1. Establish a Reservoir Matrix Attribute Model

The target layer structure in the research area is gentle, and natural faults and fractures are not developed. The burial depth of the target layer is between 1000 m and 1100 m. The Chang 6_1 Formation belongs to the sedimentary environment of the delta front. In the target layer of the study area, most of the reservoirs belong to the microfacies of underwater distributary channels. The thickness of the formation is 35–45 m, the average effective thickness is 13.3 m, the average porosity of the reservoir is 13.9%, and the average permeability is 2.29 mD, which belongs to a low porosity and low permeability reservoir [11].

Firstly, the reservoir matrix model was established. The study area is 50 km^2; 347 wells' geological stratification data and 3D seismic interpretation data are used, so the structural model can be constructed. On the basis of the tectonic model, the lithological interpretation data of 321 wells and the seismic inversion lithological data body are used, so the lithological model can be constructed. Under the constraint of the lithology model, 309 wells' porosity, permeability, and oil saturation logging interpretation data are used, so the reservoir attribute model can be constructed, and finally the reservoir matrix model is completed.

2.2. Establishing a Geological Model of Artificially Fractured Reservoirs

There are two main methods for geological modeling of fractured oil reservoirs: deterministic modelling and stochastic modelling. The Kriging method is a deterministic interpolation method, which can give the "best" local smooth estimation. For deterministic modeling methods, the input data can be a data volume with continuous prediction results in space [12].

Stochastic modeling is based on known geological information, guided by random functions, constrained by geological conditions, and using random simulation to generate selectable reservoir models with equal probabilities. One of the main methods is the Gaussian simulation algorithm, which requires the statistical data of the actual fracture geological information as conditional data [13,14].

Based on the unified matrix model, three different fracture geological modelling schemes are adopted, and finally a comprehensive geological model of three types of fractured reservoirs is established.

2.2.1. Random Interpolative Modelling Scheme Based on FMI Fracture Interpretation Data

In the target layer of the research area, based on the artificial fracture density interpretation curves of imaging logging in four wells, and the statistical results of imaging logging and microseismic monitoring data, a random fracture model was established by a Petrel Gaussian simulation algorithm, and finally the Scheme I fracture model was completed.

After artificial fracturing in the research area, only four wells have imaging logging data. The statistics of imaging log interpretation results show that the minimum fracture strike is 20.1°, the maximum is 114.3°, most of them are distributed between 50° and 77°, and the average value of an artificial fracture strike is 65.2°. The minimum artificial fracture inclination angle was 66.8° and the maximum was 87.1°, with most of them distributed between 77° and 87.1°, and the average value of the artificial fracture inclination angles was 83° (Table 1). And, controlled by the construction parameters of the artificial fracturing, the artificial fractures interpreted by imaging logs are developed in sandstones (Figure 1). Because the average distance between the four wells is only 144.5 m, the distance between wells is relatively small (Table 1), and the four wells have a single type of sedimentary phase at the location of fracture development. Constrained by the scarcity of fracture data after artificial fracturing, it is difficult for us to obtain statistical relationships between artificial fractures and lithology and sedimentary phases, and therefore phase-controlled fracture attribute modelling cannot be achieved. However, imaging logging fracture density interpretation curves can be used as a necessary base data for fracture modelling (Figure 2).

In the study area, analyzing the statistical results of microseismic fracture monitoring (Figure 3), the fracture strike is north-east oriented, the distribution of fracture strikes is between 63.2° and 75.1°, the average value of artificial fracture strikes is 68.7°, the distribution of fracture inclination angles ranges from 76° to 89°, and the average value of the artificial fracture inclination angles is 85.3° (Table 2).

Table 1. Imaging logging fracture interpretation data.

Well Name	Well Spacing (m)	Row Spacing (m)	Formation	Depth (m)	Dip (°)	Strike (°)
WJ1	192	93	Chang 6_1^{1-2}	1118.7	66.8	72.1
WJ2	109	35	Chang 6_1^{1-2}	1033.0	86.9	85.3
			Chang 6_1^{1-2}	1038.7	79.9	114.3
			Chang 6_1^{1-3}	1055.3	84.7	70.7
			Chang 6_1^{1-3}	1057.8	77.2	68.8
WJ3	65	54	Chang 6_1^{1-2}	1039.9	86.4	77.0
			Chang 6_1^{1-2}	1040.6	85.9	39.5
			Chang 6_1^{1-2}	1041.0	82.3	56.7
			Chang 6_1^{1-2}	1050.2	86.3	56.9
			Chang 6_1^{1-2}	1051.7	86.3	50.0
			Chang 6_1^{1-3}	1064.1	87.1	20.1
WJ4	212	63	Chang 6_1^{1-3}	1054.1	86.0	71.0
		Average			83.0	65.2

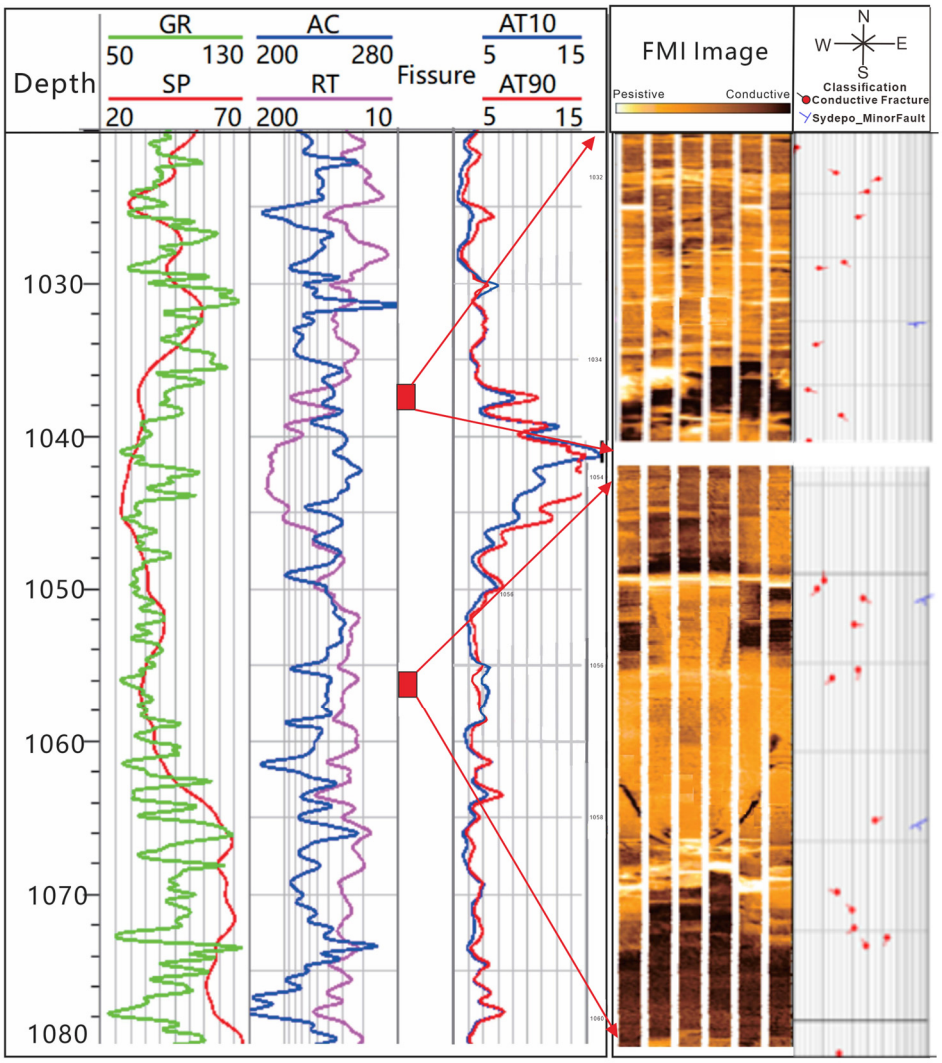

Figure 1. Imaging logging data for well WJ2.

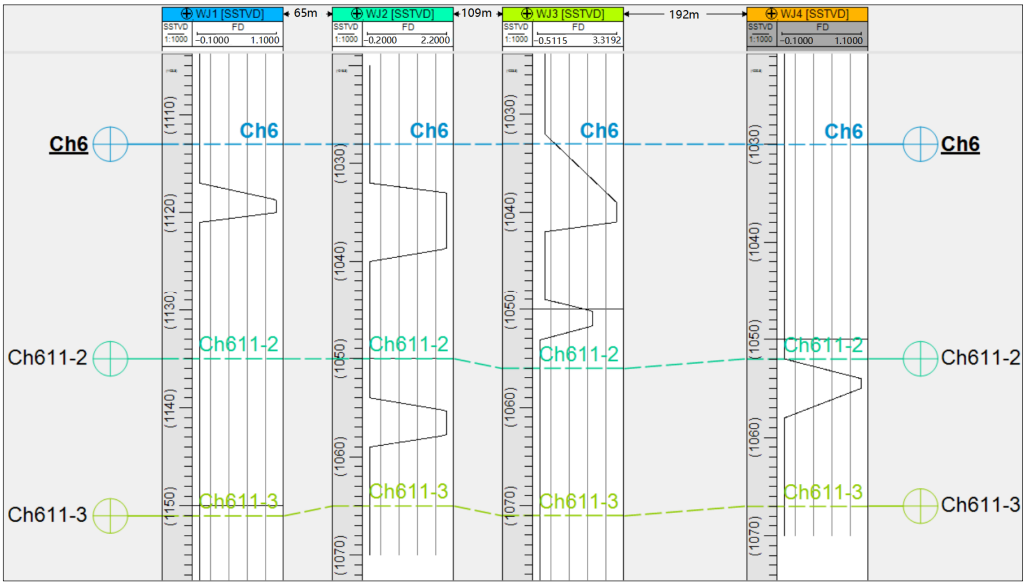

Figure 2. Fracture density interpretation curves for imaging logs after artificial fracturing.

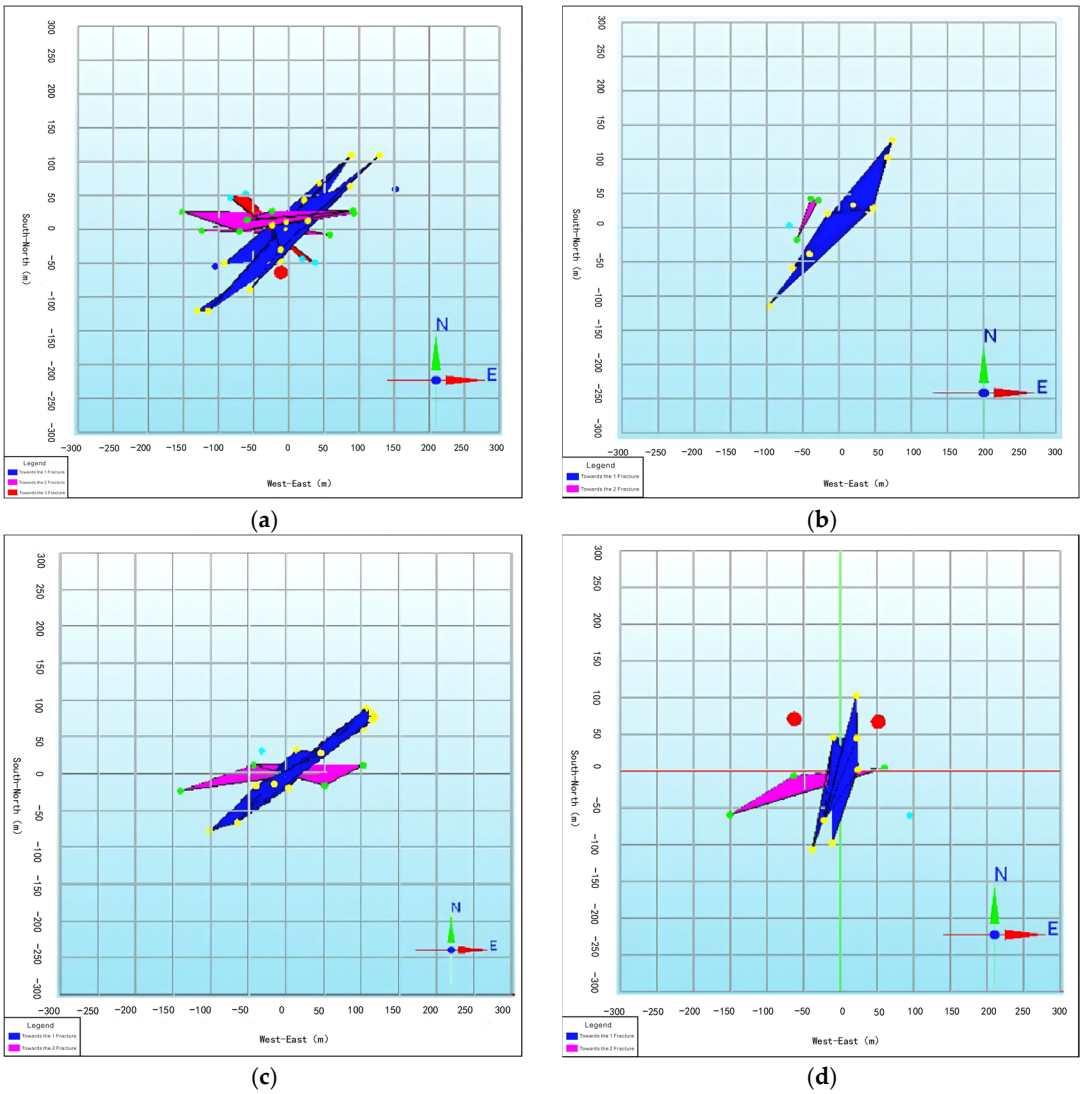

Figure 3. The three-dimensional top view of the target layer microseismic monitoring fracturing fracture in the study area: (**a**) Well WJA1; (**b**) Well WJA2; (**c**)Well WJA3; (**d**) Well WJA4.

Table 2. Statistical table of microseismic monitoring data of the target layer in the study area.

Well Name	West Wing Seam Length (m)	East Wing Seam Length (m)	Fracture Height (m)	Fracture Azimuth (°)	Strike (°)
WJA1	83.1	85.2	6.3	76	68.0
WJA2	90.1	74.0	6.6	88	75.1
WJA3	98.3	72.2	7.0	89	68.4
WJA4	74.8	92.6	5.8	88	63.2
Average	86.6	81	6.4	85.3	68.7

Microseismic fracture monitoring and imaging logging artificial fracture interpretation are in good agreement, as reflected in their statistical results. Therefore, they can be used as important condition parameters for random modelling of artificial fractures.

2.2.2. Deterministic Modelling Scheme Based on Seismic Fracture Prediction Data

Firstly, based on the 3D seismic data acquired after artificial fracturing in the study area, the pre-stack seismic fracture prediction technique was used to obtain the artificially fractured fracture intensity and azimuth data body. Then, based on the fracture intensity

curves of the four wells, and using the fracture intensity predicted by seismic inversion as the trend constraint, the Petrel deterministic fracture modelling technique was used to establish the Scheme II fracture model.

Seismic attributes such as coherent, curvature, and ant bodies are commonly used in the prediction of faults and fractures. This time, the pre-stack seismic fracture prediction technique is chosen, which has more reliable prediction results and higher prediction accuracy. Moreover, it is based on the wide-azimuth (OVT) seismic data, and then, based on the anisotropy characteristics of seismic reflection energy, the fracture intensity is finally predicted. When seismic waves propagate parallel to the direction of the fracture, the amplitude of seismic wave reflection is the strongest; when seismic waves are directed perpendicular to the direction of the fracture, the amplitude of seismic wave reflection is the weakest. Elliptic fitting of seismic reflection amplitude with azimuth is used to pre-stack seismic data. The long axis of the amplitude ellipse fitting represents the main direction of fracture development. The larger the oblateness of the ellipse, the greater the fracture development intensity. On the contrary, the smaller the oblateness of the ellipse, the smaller the fracture development strength [14]. Therefore, using pre-stack 3D seismic data with record offset, incident angle, and corresponding reflection intensity information, the direction and intensity of cracks can be predicted.

The planar pattern of the prediction results of pre-stack seismic fracture intensity is shown in Figure 4, where the anisotropy of warm shades (red and yellow) is large, which indicates a high intensity of fracture development; and the opposite is true for cool shades (blue and green). Fracturing construction wells are located in warm-toned areas, indicating greater intensity of fracture development. Their distribution controls the distribution of fractures after this artificial fracturing. The pre-stack seismic fracture prediction law is consistent with the actual situation.

In this study, based on the pre-stack 3D seismic data acquired after the construction of the artificial fracturing, the GeoEast five-dimensional seismic interpretation technology is used to obtain information, such as the direction of the artificial fracture and the fracture intensity (Figure 4). Combined with the imaging logging fracture intensity interpretation curve, it can provide reliable fracture modelling data for Scheme II.

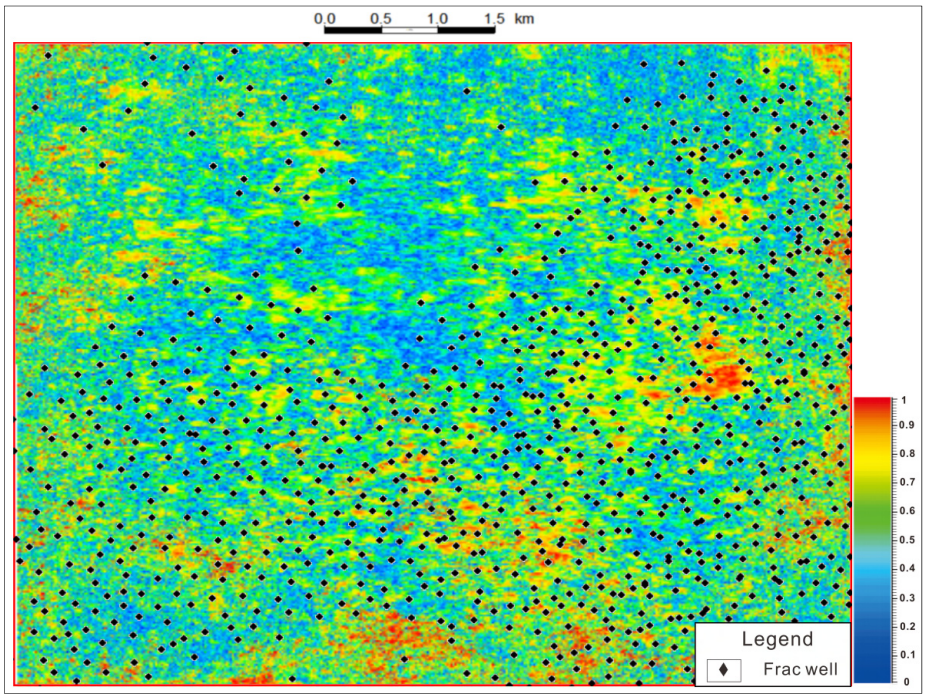

Figure 4. Prediction results of fracture intensity by seismic inversion before the target layer in the study area.

2.2.3. Deterministic Modelling Scheme Based on Rock Mechanics Artificial Fracturing Simulation Data

Firstly, based on the rock mechanics parameter model obtained from pre-stack seismic inversion, combined with the actual construction parameters of artificial fracturing, Petrel artificial fracturing simulation technology is used to simulate artificial fractures based on rock mechanics. Then, based on the fracture intensity curves of the four wells, the artificial fracture simulation results based on rock mechanics were used as the trend constraints, together with the Petrel deterministic fracture modelling technique, and finally, the Scheme II fracture model was established.

Three-dimensional data of rock mechanics parameters and in situ stress parameters with high lateral resolution can be obtained from seismic data, mainly including elastic modulus, Poisson's ratio, brittleness index, horizontal stress difference and other seismic prediction data, which can provide the necessary in situ stress model and rock mechanics parameter model for hydraulic fracturing simulation (Figure 5).

The establishment of the rock mechanics model in the study area, and the well fracturing model are set, and the fracturing simulation parameters such as proppant type and size, fracturing fluid type, and pumping program are set according to the actual construction parameters. The construction fitting is carried out according to the actual pumping program of the well, and the fracturing fracture propagation model is simulated. The simulation of the artificial fracturing fracture extension model guided by actual construction parameters can be used as the prediction results of artificial fracture fracturing and fracture creation. The simulation takes into account reservoir heterogeneity and stress anisotropy, and the simulation results can depict a real complex fracture network [15].

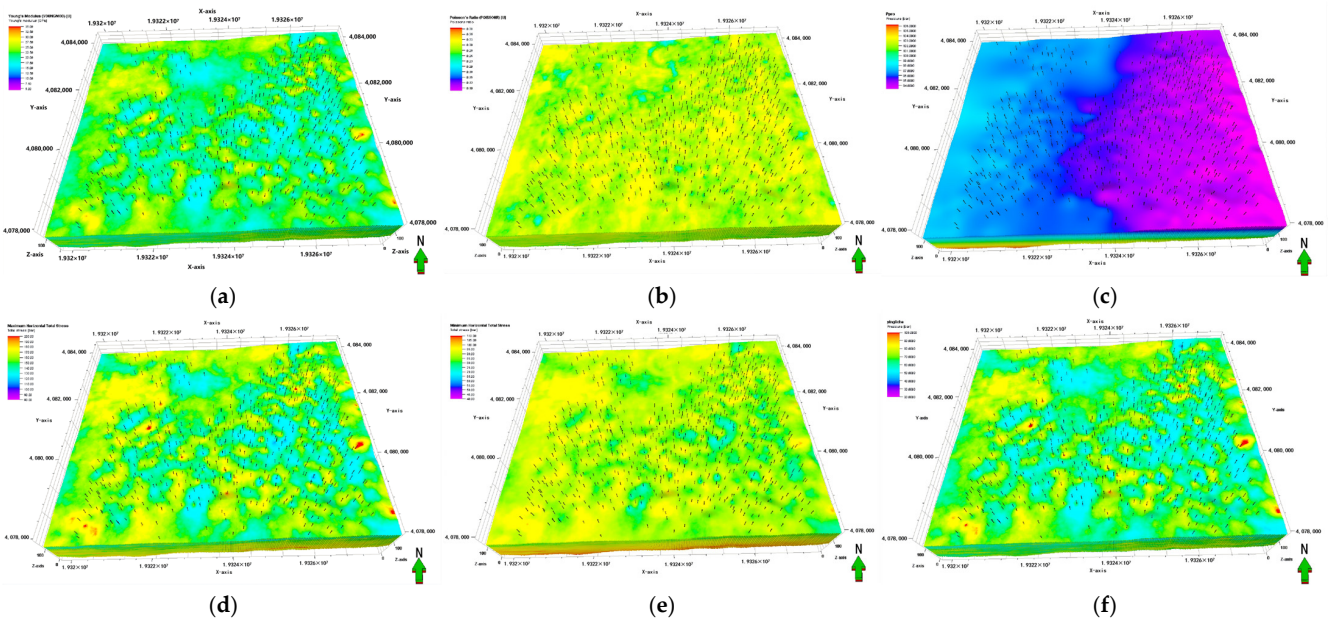

Figure 5. The model of rock elastic parameters and ground stress based on pre-stack seismic inversion: (**a**) Young's modulus earthquake prediction model; (**b**) Poisson's ratio earthquake prediction model; (**c**) Pore pressure seismic prediction model; (**d**) maximum principal stress seismic prediction model; (**e**) minimum principal stress seismic prediction model; (**f**) stress difference earthquake prediction model.

2.3. Optimal Fracture Modelling Scheme

Three artificial fracturing fractured reservoir geological models, which were established by three different schemes, were used for numerical simulation in combination with actual development history data. By comparing and analyzing the initial fitting rates, the

fracked reservoir modelling scheme applicable to the study area is preferred [16,17], and the method flow chart is shown in Figure 6.

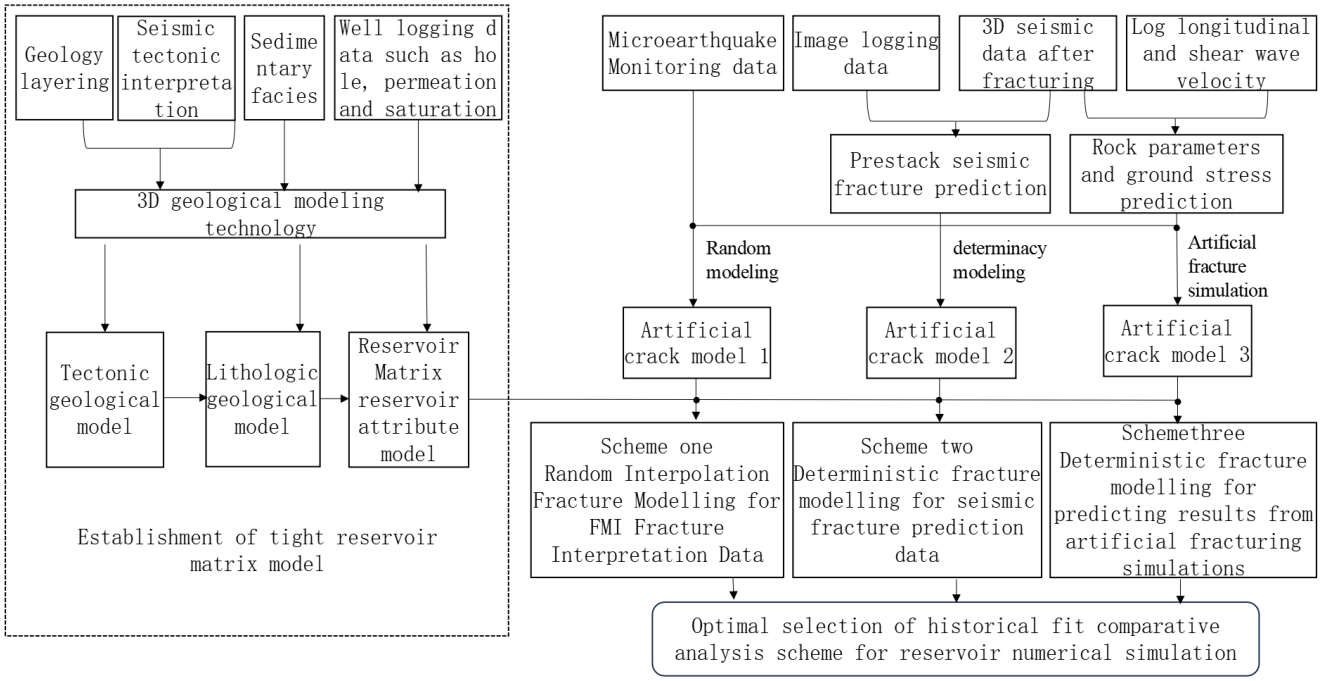

Figure 6. Flow chart of artificial fracture modeling research in tight reservoir.

3. Results

3.1. Reservoir Matrix Attribute Model

Structural models based on geological stratification as the controlling condition, and seismic data as the basis can better reflect the actual tectonic situation. Using discretized data from lithological curves, a lithological model is established based on analysis of the variation function. Using porosity, permeability, and oil saturation curve data, and employing phase-controlled attribute modeling techniques, we establish a reservoir matrix attribute model (Figure 7). Eight verification wells were selected, and these eight wells were not involved in the establishment of the attribute model. At the location of the destination layer, the values of porosity and permeability of the attribute model of these eight wells were read, and the relative error between this value and the reservoir matrix attribute model was calculated (Table 3). The statistical results show that the average relative error of porosity is 4.33%, and the average relative error of permeability is 9.76%, which is relatively small, indicating that the reservoir matrix property model is highly reliable.

Table 3. The error statistics of the wells used for validation.

Serial Number	Well Name of Validation	Porosity of Well Data (%)	Permeability of Well Data (md)	Porosity of Reservoir Matrix Model (%)	Permeability of Reservoir Matrix Model (md)	Relative Error of Porosity (%)	Relative Error of Permeability (%)
1	W1	12.49	2.35	12.22	2.28	2.16	2.93
2	W2	13.66	1.31	12.86	1.42	5.86	−8.22
3	W3	13.68	0.65	13.03	0.77	4.75	−19.17
4	W4	13.43	1.01	13.63	1.11	−1.49	−9.40
5	W5	15.07	2.89	14.58	2.75	3.25	4.81
6	W6	13.54	0.48	12.73	0.54	5.98	−12.19
7	W7	14.38	2.19	13.32	1.91	7.37	13.08
8	W8	16.06	3.54	15.46	3.24	3.74	8.29
average		14.04	1.80	13.48	1.75	4.33	9.76

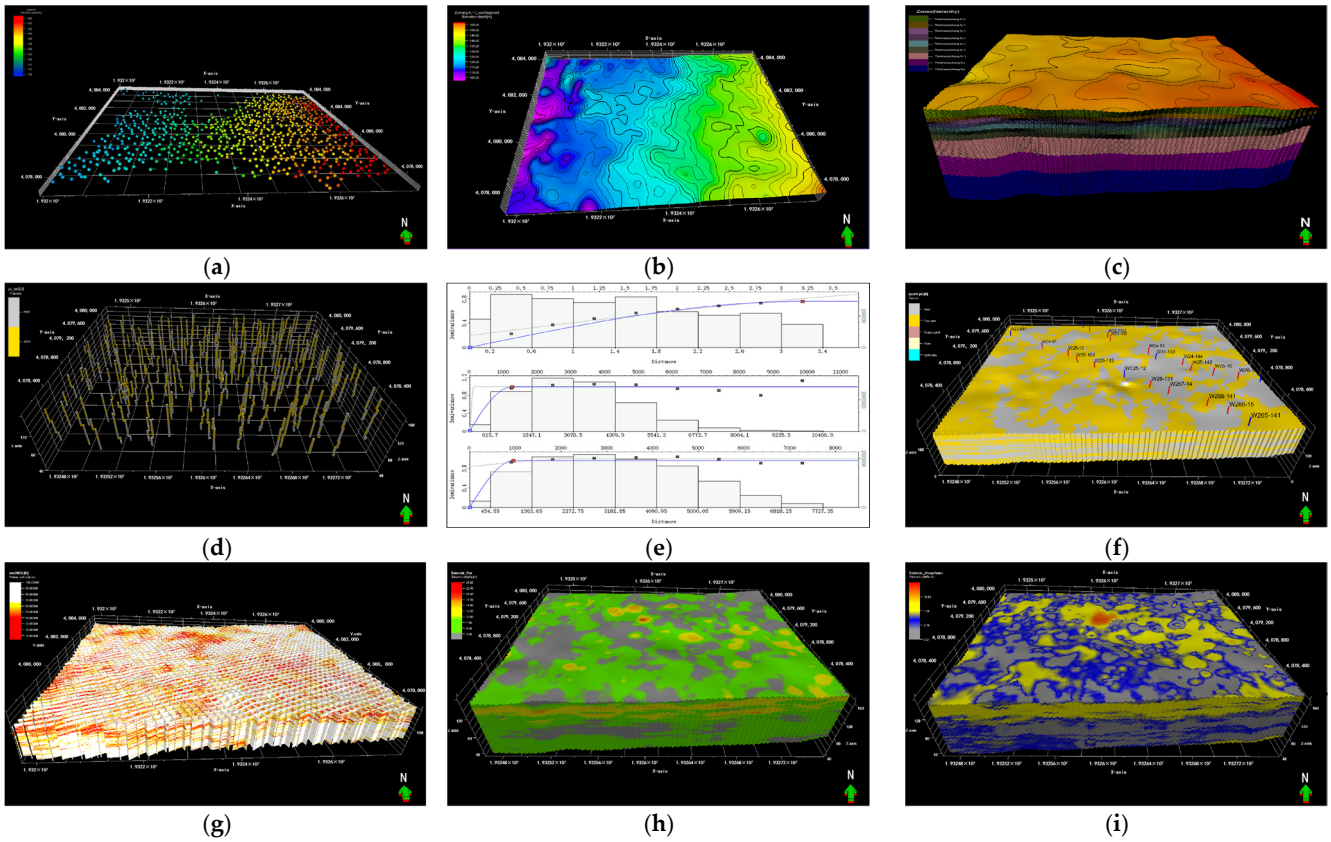

Figure 7. Establishment of the reservoir matrix property model. (**a**) Geological stratification; (**b**) surface; (**c**) structure model; (**d**) discretization of lithologic curves; (**e**) discretization of lithologic curves; (**f**) lithologic model; (**g**) oil-saturation model; (**h**) permeability model; (**i**) porosity model.

3.2. Geological Model of Artificial Fractures

3.2.1. Random Interpolation Fracture Model Based on FMl Fracture Interpretation Data

The fracture density curve, combined with the spatially averaged statistical characteristics of the fracture, is determined by imaging logging and microseismic statistics. On this basis, using random modelling method, the DFN fracture prediction model of Scheme I can be obtained (Figure 8). By analyzing the fracture prediction plane characteristics, the direction of fractures in the study area is dominated by north-east direction, with the average length of fractures being 168 m and the height of cracks being 6.5 m, which is in line with the statistical characteristics of fractures in the study area.

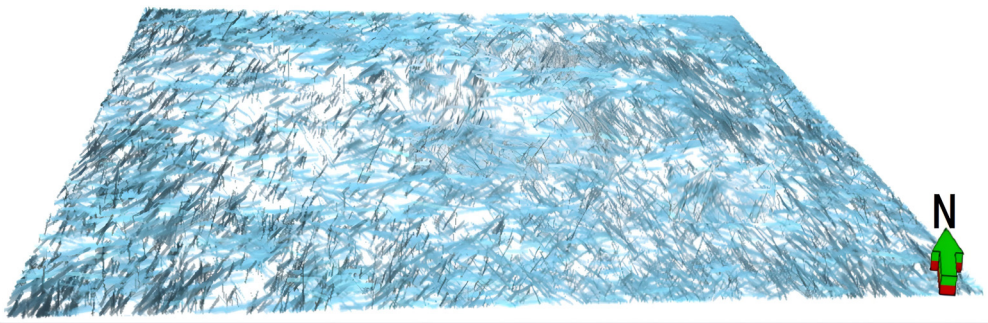

Figure 8. Random-simulated DFN fracture prediction model.

3.2.2. Deterministic Fracture Modelling Based on Seismic Fracture Prediction Data

From the fracture data predicted by the pre-stack seismic inversion, a DFN fracture prediction model can be built for Scheme II (Figure 9). By the fracture prediction plane

characteristics, the fracture direction is mainly in the north-east direction; the average length of the fracture is 170 m, and the average height of the fracture is 7 m, which is in line with the statistical characteristics of the fractures in the study area, and the plane distribution law is locally different from Scheme I. Fracture intensity is higher in areas where fracturing construction wells are distributed; however, in the northern part of the study area, where fracturing construction wells are sparsely distributed, it has less fracture intensity. Fracture distribution after artificial fracturing is controlled by the distribution of fracturing construction wells, and the fracture prediction law is consistent with the actual situation.

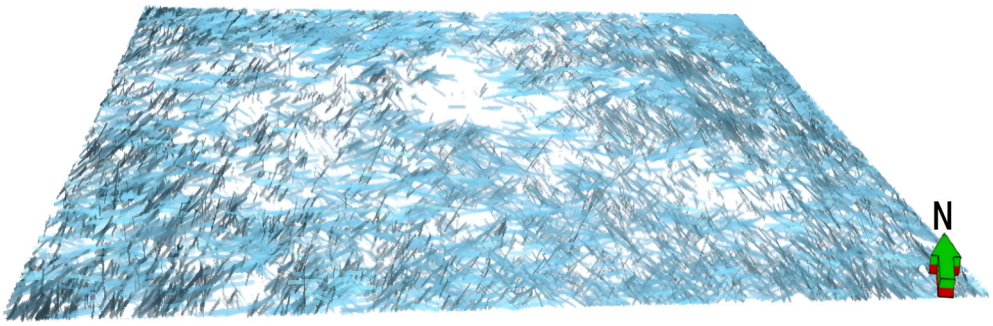

Figure 9. DFN fracture prediction model for earthquake prediction.

3.2.3. Deterministic Fracture Model Based on Rock Mechanics Artificial Fracturing Simulation Prediction Results

The artificial fracture prediction results obtained by Petrel's artificial fracturing simulation technology (Figure 10), combined with the imaging logging fracture density curves, can provide fracture information for Scheme III, which establishes the artificial fracturing fracture reservoir physical properties model. The predicted fracture model has an average fracture length of 172 m and an average fracture height of 6.2 m. The fracture simulation results are consistent with the microseismic monitoring statistics. Fracture simulation results in a regular planar distribution, which is significantly controlled by the location of the fracking construction wells.

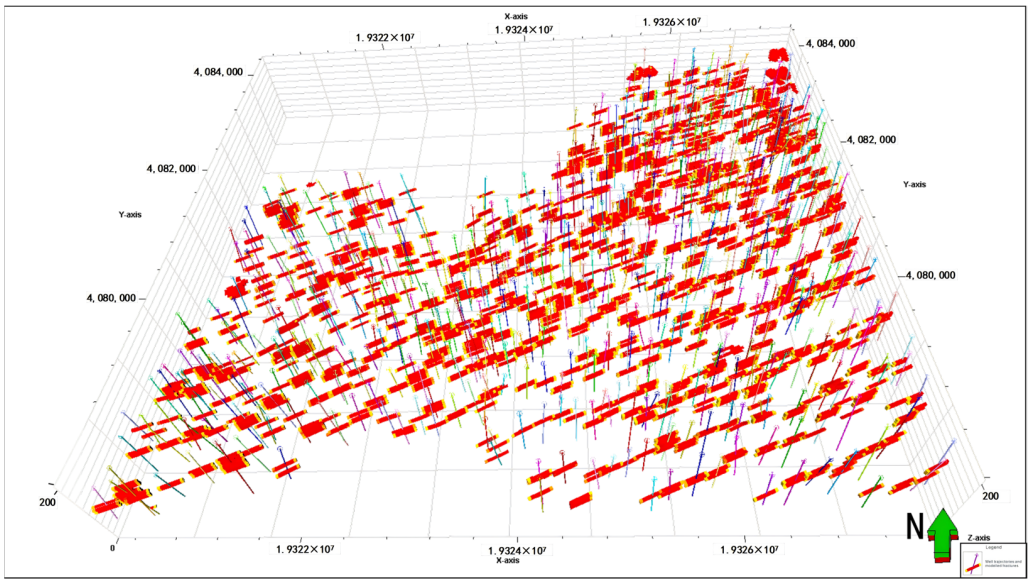

Figure 10. Fracture prediction model for artificial fracturing simulation.

3.3. Optimization of Artificial Fracture Reservoir Geological Modeling Scheme in Tight Reservoir

Three crack models were developed for the three scenarios and their planar patterns were analyzed. The overall law of their description of artificial fractures is consistent with geological understanding, that is, the fracture direction is mainly north to east, and the fracture length and height are in line with statistical law, which is based on the fracture monitoring data.

At the same time, the fracture models established by the three scenarios in the prediction of the plane details have obvious differences: Scenario 1 statistical data control under the stochastic modelling fracture prediction results (Figure 8) are less correlated with the distribution location of the fracturing construction wells. Therefore, the distribution density characteristics of fractures do not change much. In the second scenario, in the fracture model established by the pre-stack seismic inversion fracture prediction results (Figure 9), there is a sparse area of fracture development in the north of the working area, which is consistent with the sparse area of fracturing construction wells. However, at the same time, the predicted fracture density in the north-west corner of the site is locally inconsistent with the distribution of the fractured wells. Scenario III is the artificial fracturing simulation fracture model (Figure 8), which is based on the seismic prediction of the in situ stress and rock lithology parameter model, and the artificial fracture simulation results obtained by adopting the actual fracturing construction parameters, which are not only in line with the statistical law of the distribution of fracture planes, but also can accurately reflect the distribution of artificial fracturing fracture and the distribution of the fracturing construction wells.

Three fractured reservoir geological models were established by the three schemes, and their initial fitting rates for reservoir numerical simulation were compared and analyzed (Figure 10). The fractured reservoir geological model established by the third modelling scheme, which was based on the fracture prediction results of the artificial fracturing simulation based on rock mechanics, had the highest initial historical fitting rate of 88.44%. The first scheme is based on microseismic monitoring parameters. It is also based on the fracture prediction information established using stochastic methods, and thus the fractured reservoir geological model established, which has an initial fit rate of 75.76% for the numerical simulation of the reservoir. The second scheme is based on the fracture prediction results from pre-stack seismic data, and the initial fitting rate of the numerical simulation is 77.51%.

The three schemes establish three fractured reservoir geological models, and analyze their initial fitting rates for numerical simulation of the reservoir (Figure 11). The third modelling scheme is established based on the artificial fracturing simulation fracture prediction data of rock mechanics, and it has the highest initial historical fit rate of 88.44%. The first scheme, which is based on imaging logging interpretation data, using a stochastic method, established fracture prediction information. It establishes a geological model of fractured reservoir, whose initial fitting rate of reservoir numerical simulation is 75.76%. The second scheme, which is based on pre-stack seismic fracture prediction data, establishes a reservoir geological model whose reservoir numerical simulation initial fitting rate is 77.51% (Table 4).

Table 4. Statistical table of initial fitting rate of fractured reservoir models with different schemes.

Modeling Scheme	Model Data Source			Modeling Method	Fit Rate (%)
Scheme I	Fracture intensity curves and microseismic fracture monitoring information			Stochastic modeling	75.76
Scheme II	Fracture intensity curves and microseismic fracture monitoring information	Earthquake fracture prediction		Deterministic modeling	77.51
Scheme III	Fracture intensity curves and microseismic fracture monitoring information	Earthquake elastic parameters and ground stress prediction	Rock mechanics fracturing simulation	Deterministic modeling	88.44

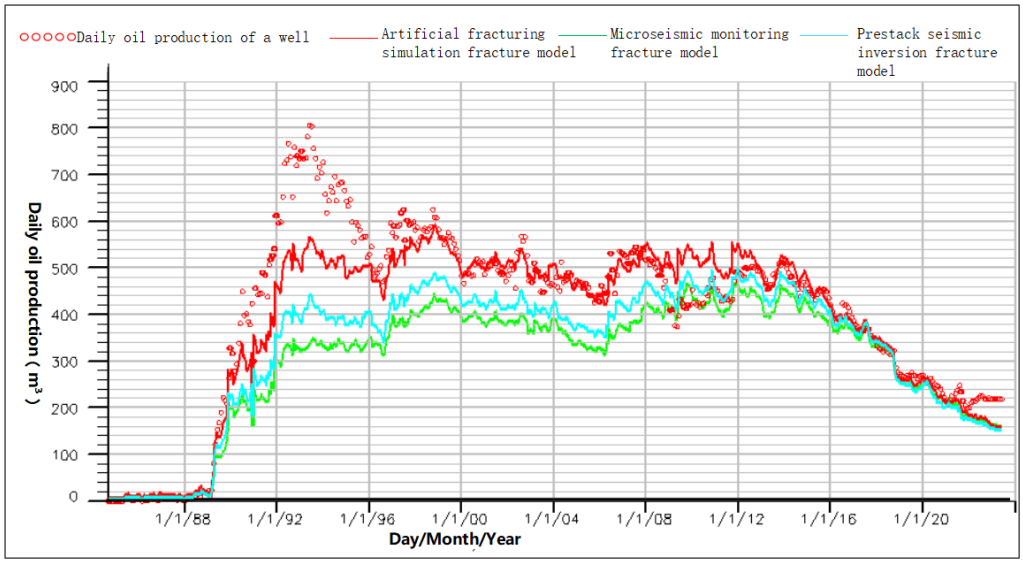

Figure 11. Comparison of initial fitting rates of reservoir numerical simulation for fracture reservoir geological models established by different schemes.

4. Discussion

Currently, there are fewer studies dedicated to the prediction and characterization of artificial fractures, and through the results of this comparison of three types of artificial crack prediction and description schemes, the reasons for the variability of the three prediction schemes are initially discussed.

The initial fitting rate of the reservoir in Scheme I is low, which may be because the method of fracture prediction used in this scheme is not applicable [18]. The well data in the study area are not uniformly distributed, with only four fracture intensity datasets, and the four distribution locations are concentrated, which cannot achieve more reliable constraints such as phase control in random simulation. The artificial fracture is mainly controlled by the distribution of construction wells; random algorithm cannot effectively reflect the special law of artificial fracture plane distribution.

The initial fitting rate of the reservoir in Scheme II is relatively low, and it may be due to the insufficient resolution of seismic fracture prediction adopted in Scheme II [19]. Artificial fracture size and density are relatively small, affected by the resolution of seismic data, although the plane law of seismic fracture prediction results is accurate but its resolution is relatively low.

The reason for the relatively high fitting rate of Scheme III is, firstly, that the crack prediction method can reflect the specificity of the planar distribution of artificial cracks. The fracture prediction is based on the artificial fracture simulation method, which uses the actual engineering parameters, pre-stack seismic elasticity, and in situ stress inversion prediction results as the trend control. Secondly, the prediction results of fracture length, width, height, etc., of the artificial fracturing simulation are controlled by microseismic fracture monitoring data, which can reflect the accuracy of the actual artificial fractures. These may be some of the reasons why the program is suitable for the prediction of artificial fractures.

The method of obtaining fracture information data after artificial fracturing is limited, and due to the lack of actual data in this research area, there are still some imperfections in this study, which are expected to be gradually improved by subsequent studies, specifically the following points:

1. Any fracture prediction results can be used as constraint data for fracture modelling, combined with fracture intensity curves to build a fracture model. In this study, only three methods have been used for comparison, and when data are abundant, more fracture modelling schemes can be established for comparative studies.

2. In this study, the role of the interlayer in controlling the development of artificial fractures was not considered. In the next study, it is necessary to include the thickness information of the interlayer in the modelling of artificial fractures, and a more accurate model of artificial cracks will be obtained.
3. The study is limited by the actual geological and objective conditions. The results and conclusions of the study are only applicable to geological research areas that have similar geological and objective conditions as the research area.

5. Conclusions

This study compares and analyzes the initial fitting rates of the fractured reservoir models of different schemes. Option 3, a fractured reservoir geological model based on rock mechanics fracturing simulation, which can characterize the fractured reservoir features in post-low-permeability reservoirs, is preferred. The following understandings are obtained during the research process:

(1) Based on different data sources and fracture prediction methods, there are various modeling schemes for fracture reservoir geological models. Due to the differences in the geological conditions of the target layer, the applicability of each modeling scheme is also different.
(2) By comparing and analyzing the fitting rates of different schemes, the best geological modelling scheme for fractured reservoirs in the destination layer of the study area was preferred.
(3) Three fracture scenarios were analyzed, in which the deterministic fracture modelling method was established based on the fracture intensity curves, using the predicted results of the artificial fracturing simulation as constraints, and it is the most suitable method for the description of the post-artificial fracturing fractures in the study area.

Author Contributions: Conceptualization, Y.W. and X.Z.; methodology, Y.W. and J.Z.; software, X.Z. and L.Z.; validation, Y.W. and J.Z.; formal analysis, X.Z.; investigation, Y.Z. and H.W.; resources, L.Z. and Y.Z.; data curation, H.W. and R.L.; writing—original draft preparation, X.Z.; writing—review and editing, Y.W.; visualization, X.Z. and R.L.; supervision, Y.W.; project administration, Y.W. and J.Z.; funding acquisition, Y.W. All authors have read and agreed to the published version of the manuscript.

Funding: This research was funded by the Research on Scale Storage and Production Increase of Continental Shale Oil and Exploration and Development Technology-Research on Key Technology of Geophysical Modelling of Continental Shale Oil, grant number 2023ZZ15YJ02, the Natural Science Foundation of Chongqing, China, grant number cstc2021hcyj-msxmX0984, and the Talent Program "Package System" Project funded by the Municipal of Chongqing, China, grant number cstc2024ycih-bgzxm0064.

Data Availability Statement: The original contributions presented in the study are included in the article, further inquiries can be directed to the corresponding author.

Conflicts of Interest: Authors Yonggang Wang, Jie Zhang and Yali Zeng were employed by the Research Institute of Exploration and Development, Changqing Oilfield Company, PetroChina. The remaining authors declare that the research was conducted in the absence of any commercial or financial relationships that could be construed as a potential conflict of interest.

References

1. Darisma, D.; Mukuhira, Y.; Okamoto, K.; Aoyogi, N.; Uchide, T.; Ishibashi, T.; Asanuma, H.; Ito, T. Building the fracture network model for the Okuaizu geothermal field based on microseismic data analysis. *Earth Planets Space* **2024**, *76*, 107. [CrossRef]
2. Mehdipour, V.; Rabbani, A.R.; Kadkhodaie, A. Geological modeling of diagenetic logs of the Sarvak reservoir in Dezful Embayment, southwestern Iran: Implications for geostatistical simulation and reservoir quality assessment. *J. Pet. Explor. Prod. Technol.* **2023**, *13*, 2083–2107. [CrossRef]
3. Dershowitz, B.; LaPointe, P.; Eiben, T.; Wei, L. Integration of discrete feature network methods with conventional simulator approaches. *SPE Reserv. Eval. Eng.* **2000**, *3*, 165–170. [CrossRef]

4. Sarda, S.; Jeannin, L.; Basquet, R.; Bourbiaux, B. Hydraulic characterization of fractured reservoirs: Simulation on discrete fracture models. *SPE Reserv. Eval. Eng.* **2002**, *5*, 154–162. [CrossRef]
5. Jian, W.; Yuanhui, S.; Bin, W.; Yongjun, W.; Lei, X.; Chunmeng, D. 3D geological modeling of fractured volcanic reservoir bodies in Block DX18 in Junggar Basin, NW China. *Pet. Explor. Dev.* **2012**, *39*, 99–106.
6. Hao, S.; Zhengdong, L.; Zhang, D.; Li, J.; Zhang, Z.; Ju, B.; Li, Z. Dynamic and static comprehensive prediction method of natural fractures in fractured oil reservoirs: A case study of Triassic Chang 63 reservoirs in Huaqing Oilfield, Ordos Basin, NW China. *Pet. Explor. Dev.* **2017**, *44*, 972–982.
7. Qiu, X. Application of 3D Geological Modeling and Numerical Simulation Technology of Computer in Modern Reservoir Development. *JPCS* **2020**, *1574*, 012053. [CrossRef]
8. Xing, S. Fine Geology Research in Late Stage of Oilfield Development Based on Computer 3D Geological Modeling Technology. *J. Phys. Conf. Ser.* **2020**, *1574*, 012013. [CrossRef]
9. Li, W.; Guo, Z.X.; Chun, H.X. Microseismic Monitoring of Failure Mechanisms in Extra Thick Coal Seam Surrounding Rock. *Geotech. Geol. Eng.* **2024**, *42*, 2403–2423. [CrossRef]
10. He, Z.; Sun, J.; Guo, P.; Wei, H.; Lyu, X.; Han, K. Construction of carbonate reservoir knowledge base and its application in fracture-cavity reservoir geological modeling. *Pet. Explor. Dev.* **2021**, *48*, 824–834. [CrossRef]
11. Shi, Q.; Li, C.; Wang, S.; Li, D.; Wang, S.; Du, F.; Qiao, J.; Cheng, Q. Effect of the depositional environment on the formation of tar-rich coal: A case study in the northeastern Ordos Basin, China. *J. Pet. Sci. Eng.* **2022**, *216*, 110828. [CrossRef]
12. Dincel, A.T.; Tural-Polat, S.N.; Afacan, M.O. Numerical simulation for fractional optimal control problems via euler wavelets. *Phys. Scr.* **2024**, *99*, 095241. [CrossRef]
13. Chen, L.; Song, Y.; Duan, F.; Hu, Z.; Chu, W.; Liu, Z. Wave propagation analysis of the overhead conductor rail system based on numerical simulation and full-scale experiment. *Mech. Mach. Theory* **2024**, *202*, 105769. [CrossRef]
14. Liu, Z.; Ma, X.; Chi, J.; Chen, Y.; Wang, C. Centrifuge model tests and numerical simulation on ground-borne vibration propagating and vibration reduction scheme for tunnel inner structure. *Tunn. Undergr. Space Technol.* **2024**, *153*, 105996. [CrossRef]
15. Vermeer, G.J.O. Processing with offset-vector-slot gathers. In *SEG Technical Program Expanded Abstracts 2000*; SEG: Tulsa, OK, USA, 2000; pp. 5–8.
16. Zou, Y.; Li, Y.; Yang, C.; Zhang, S.; Ma, X.; Zou, L. Fracture propagation law of temporary plugging and diversion fracturing in shale reservoirs under completion experiments of horizontal well with multi-cluster sand jetting perforation. *Pet. Explor. Dev.* **2024**, *51*, 715–726. [CrossRef]
17. Duan, Y.; Wu, Y. Distribution and formation of Mesozoic low permeability underpressured oil reservoirs in the Ordos Basin, China. *J. Petrol. Sci. Eng.* **2020**, *187*, 106755. [CrossRef]
18. Dang, Y.; Zhang, Y.; Wu, B.; Li, H.; Gao, J. An efficient method of predicting S-wave velocity using sparse Gaussian process regression for a tight sandstone reservoir. *J. Appl. Geophys.* **2024**, *229*, 105480. [CrossRef]
19. Zhang, K.; Ma, X.; Li, Y.; Wu, H.; Cui, C.; Zhang, X.; Zhang, H.; Yao, J. Parameter prediction of hydraulic fracture for tight reservoir based on micro-seismic and history matching. *Fractals* **2018**, *26*, 1840009. [CrossRef]